Eksakta : Berkala Ilmiah Bidang MIPA
VOLUME 27 NO 04 2026, pp 637-658
ISSN : Print 1411-3724 — Online 2549-7464
DOI : https://doi.org/10.24036/eksakta/vol27-iss04/698

Eksakta
Berkala Ilmiah Bidang MIPA
http://www.eksakta.ppj.unp.ac.id/index.php/eksakta

Article

Identification of Fault Structures Using First Horizontal Derivative and Second Vertical Derivative Analysis of Gravity Data in the Sumedang Area, West Java

Laudrien Natarissa[1*], Noor Muhammad Indragiri[2], Mochamad Ervan[2], Hesty Sampeliling[2], Budy Santoso[1]

[1]Department of Geophysics, Faculty of Mathematics and Natural Science, Universitas Padjadjaran, Bandung, Indonesia
[2]Geological Agency, Ministry of Energy and Mineral Resources, Geological Survey Center

Article Info

Article history :
Received May 29, 2026
Revised July 20, 2026
Accepted July 27, 2026
Published August 30, 2026
In Press

Keywords :
Gravity,
spectral analysis,
FHD-SVD,
fault structures,
Sumedang

Abstract. Sumedang is a region with complex tectonic activity, making the identification of subsurface fault structures essential for understanding geological conditions and potential geohazards. This study aims to identify subsurface fault structures in Sumedang, West Java, using gravity data through First Horizontal Derivative (FHD) and Second Vertical Derivative (SVD) analysis. A total of 271 Bouguer anomaly data points were analyzed through regional–residual anomaly separation, spectral analysis, derivative analysis, and 2D forward modeling. Spectral analysis estimated average regional and residual depths of 9188.13 m and 2564.5 m, respectively. Fault interpretation was conducted based on the relationship between the SVD zero points and the extreme values of the FHD, supported by residual anomaly contrasts. The results indicate reverse faults, normal faults, and strike-slip faults with reverse components. The identified structures include the Baribis Fault on lines 5 and 7, the Rajamandala Fault on line 1, and the Cimanuk Fault on line 5, consistent with the Java–Bali–NTB active fault database. The 2D modeling results reveal the presence of younger sediment, older sediment, and basement. The study demonstrates that the combination of FHD and SVD analysis is effective for identifying subsurface fault structures in tectonically complex regions such as Sumedang.

Corresponding Author :
Laudrien Natarissa
Department of Geophysics, Faculty of Mathematics and Natural Science,
Universitas Padjadjaran, Bandung, Indonesia
Email : laudrienntarissa22@gmail.com

1. Introduction

Indonesia is a tectonically active region with a high level of geological vulnerability due to the interaction of three major tectonic plates: the Indo-Australian, Eurasian, and Pacific plates. The island of Java has been shaped by the ongoing subduction of the Indo-Australian Plate beneath the Eurasian Plate, a process that continuously generates crustal deformation in the form of folds, faults, and complex fracture zones. This tectonic activity plays a significant role in generating shallow to intermediate-depth earthquakes on Java [1–4]. Recent studies indicate that deformation dynamics in West Java are strongly influenced by the interaction between the subduction system and structurally associated active local faults [3]. Furthermore, the integration of modern geophysical data, such as high-resolution gravity and GNSS, has significantly enhanced our understanding of active tectonic dynamics [5]. Therefore, studies of subsurface structures are crucial for understanding regional geological evolution and supporting efforts to mitigate geological hazards [4],[6].

Sumedang Regency is one of the regions in West Java located within a complex tectonic setting influenced by subduction activity. This region is affected by several active faults, such as the Baribis, Cimandiri, Rajamandala, Cileunyi–Tanjungsari, and Cimanuk faults, which are part of the active fault system in western Java [7–8]. Recent research findings indicate that the distribution of faults in West Java strongly correlates with patterns of gravity anomalies and modern seismic activity, suggesting that most of these faults remain active [9]. Additionally, volcanic activity, particularly from Mount Tampomas, has contributed to the stratigraphic and lithological complexity of the study area [8],[10]. The interaction between tectonic processes and volcanism has resulted in high lithological heterogeneity, ranging from volcanic rocks and sediments to alluvial deposits [7]. Such lithological variability may obscure the surface expression of tectonic structures and complicate the identification of fault zones using geological observations alone. Therefore, subsurface geophysical investigations are required to better delineate fault-related structures in the Sumedang region.

This structural and lithological complexity makes subsurface conditions in the Sumedang region difficult to interpret based solely on surface geological observations. Therefore, geophysical approaches serve as an effective method for indirectly identifying subsurface structures. The gravity method is one of the most widely used geophysical methods because it can detect variations in rock density associated with geological structures such as faults, folds, and intrusions [11–12]. In recent years, the use of derivative techniques on gravity data has advanced significantly and has proven capable of enhancing the resolution of geological structure interpretation [13].

In gravity data processing, derivative analysis such as the First Horizontal Derivative (FHD) and Second Vertical Derivative (SVD) are highly effective techniques for highlighting density contrast boundaries and identifying fault structures [3],[14]. FHD is used to detect lateral changes in gravity anomalies associated with geological structure boundaries, while SVD functions as a high-frequency filter capable of enhancing local anomalies and shallow structures [11],[15–16]. Additionally, the relationship between the maximum and minimum SVD values can be used to interpret fault types, such as normal, reverse, and strike-slip faults [17–20].

Recent studies have demonstrated the effectiveness of gravity derivative analysis for identifying subsurface fault structures. In the Way Panas geothermal area, Wonosobo, FHD and SVD analyses successfully identified several fault structures controlling the geothermal system [21]. Similarly, gravity studies in the Mount Ciremai geothermal area revealed fault structures and geothermal reservoir zones controlled by subsurface geological features [12]. In southern Sumbawa, SVD analysis proved effective in delineating fault locations and characteristics based on gravity anomalies [17]. In the Sumedang region, GGMplus gravity data have been utilized to identify regional geological structures around Mount Tampomas [10]. However, these studies mainly focused on regional structural mapping or geothermal exploration and did not specifically investigate subsurface fault characterization using an integrated FHD–SVD approach validated against active fault data.

Despite the successful application of FHD and SVD analyses in geothermal and regional structural studies, investigations focusing on subsurface fault identification in the Sumedang region remain limited. Furthermore, comparisons between gravity-derived fault interpretations and active fault maps compiled by the Geological Survey Center (PSG) have rarely been incorporated into similar studies. Therefore, this study integrates FHD–SVD analyses, correlation with PSG active fault data, and 2D forward modeling to provide a more comprehensive interpretation of subsurface fault geometry in the Sumedang area.

Accordingly, this study aims to identify subsurface fault structures in the Sumedang region using gravity data through the integration of First Horizontal Derivative (FHD), Second Vertical Derivative (SVD), and 2D forward modeling. The results are expected to improve the understanding of subsurface structural geometry and provide supporting information for geological hazard assessment in the region.

2. Materials and Methods

2.1. Study Area

Measurements were conducted in the Sumedang region at 271 observation points. The Bouguer anomaly data, which had undergone correction processes, were subsequently overlaid to analyze the distribution of the measurement data, as shown in Figure 1.

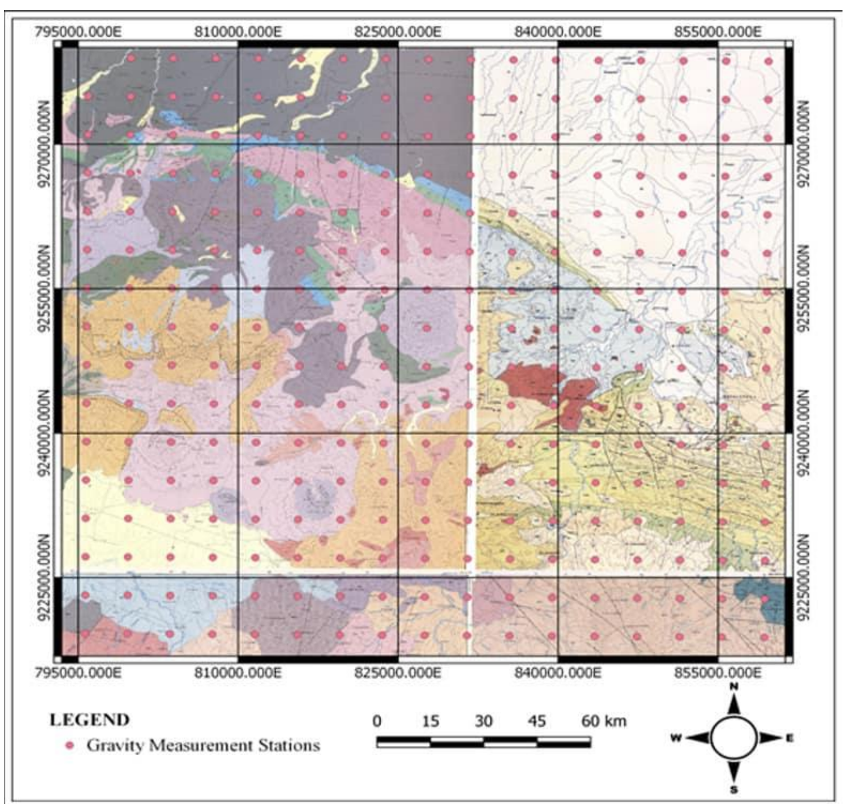

Figure 1. Gravity measurement stations map

The gravity measurement data are presented in Table 1.

Table 1. Bouguer anomaly data

Gravity Measurement Stations	X	Y	Bouguer Anomaly (mGal)
1	795636.5	9219212	21.219
2	799616.6	9219189	20.350
3	803596.8	9219166	16.678
4	807577	9219142	18.115
5	811557.5	9219118	21.702
6	815538	9219094	23.909
7	819518.6	9219069	25.196
8	823499.4	9219044	31.732
9	827480.3	9219019	36.621
10	831461.3	9218994	33.961
:	:	:	:
:	:	:	:
271	859733.6	9278596	22.241

2.2. Data Processing

The gravity measurement data were first subjected to a series of corrections to obtain Bouguer anomaly values that more accurately represent subsurface density variations. These correction stages included drift, tide, latitude, free-air, and Bouguer corrections, resulting in complete Bouguer anomalies ready for further analysis [11–12]. The subsequent data processing stages included spectral analysis, derivative analysis, fault structure identification, and two-dimensional (2D) forward modeling [4],[14].

Spectral analysis was conducted to separate regional and residual anomaly components based on signal frequency characteristics. This stage included data slicing, Fourier transformation, and the construction of spectral curves between the wave number (k) and the logarithm of amplitude (ln A). In the frequency domain, the spectral function F(k) was analyzed with respect to the spatial function f(x), resulting in a wave number value used as the boundary separating regional anomalies (low frequency) from residual anomalies (high frequency). This value was then used as a parameter in the filtering process [15–16],[24–25].

The separation of regional and residual anomalies was performed using a Gaussian filter, which was selected for its ability to produce smoother separation results and minimize noise effects compared to other filters [11][16]. In addition, the depth estimation of anomaly sources was carried out through spectral analysis by interpreting the slope (gradient) of the ln(A) versus k curve. This gradient is directly correlated with the depth of the anomaly source and can therefore be used to estimate the depths of regional and residual anomalies [4],[24].

Furthermore, derivative analysis using the First Horizontal Derivative (FHD) and Second Vertical Derivative (SVD) were applied to the residual anomaly map. This analysis aimed to enhance density contrast boundaries and highlight linear patterns indicating the presence of fault structures [3],[13-14]. FHD was used to identify lateral changes in anomaly gradients by calculating the first derivative in the horizontal directions (x and y). Mathematically, the FHD is expressed as:

$$FHD = \sqrt{\left(\frac{\partial g}{\partial x}\right)^2 + \left(\frac{\partial g}{\partial y}\right)^2} \quad (1)$$

The maximum values of the FHD generally indicate density contrast boundaries associated with geological structures such as faults or lithological contacts. Meanwhile, the SVD was used to enhance vertical density contrast boundaries, particularly for emphasizing shallow anomalies. The SVD is also effective in detecting fault structures characterized by changes in extreme values and zero points (zero crossings). Mathematically, the SVD follows Laplace's equation as follows:

$$\nabla^2 \cdot \Delta g = \frac{\partial^2 \Delta g}{\partial x^2} + \frac{\partial^2 \Delta g}{\partial y^2} + \frac{\partial^2 \Delta g}{\partial z^2} = 0 \tag{2}$$

$$\frac{\partial^2 \Delta g}{\partial z^2} = -\left(\frac{\partial^2 \Delta g}{\partial y^2} + \frac{\partial^2 \Delta g}{\partial x^2}\right) \tag{3}$$

The combined analysis of FHD and SVD enables the separation of overlapping anomalies, allowing geological structure interpretation to be carried out more accurately [4],[11,][17]. Fault structure identification was performed by integrating the results of the FHD and SVD analysis with the regional geological map. At this stage, profile slicing was conducted on the residual anomaly, FHD, and SVD maps to analyze the correlation between the curves. The indication of fault structures is characterized by maximum or minimum values on the FHD curve associated with zero values on the SVD curve [26–27].

$$\left(\frac{\partial^2 g}{\partial z^2}\right)_{max} > \left|\left(\frac{\partial^2 g}{\partial z^2}\right)\right|_{min} \text{ Normal Fault} \tag{4}$$

$$\left(\frac{\partial^2 g}{\partial z^2}\right)_{max} < \left|\left(\frac{\partial^2 g}{\partial z^2}\right)\right|_{min} \text{ Reverse Fault} \tag{5}$$

$$\left(\frac{\partial^2 g}{\partial z^2}\right)_{max} \approx \left|\left(\frac{\partial^2 g}{\partial z^2}\right)\right|_{min} \text{ Strike-Slip Fault} \tag{6}$$

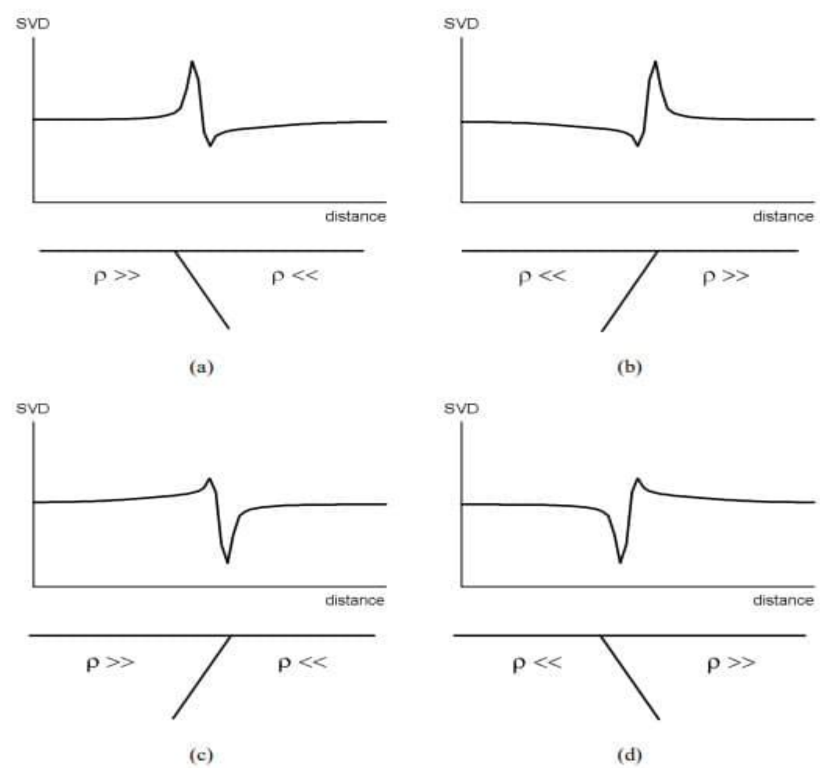

Figure 3. Relationship between density contrast and the SVD profile [27]

In addition, fault classification was carried out by comparing the maximum and minimum values of the SVD response. Normal faults are indicated when the maximum SVD value exceeds the minimum value, whereas reverse faults are identified when the maximum value is lower than the minimum value. Faults with relatively similar maximum and minimum SVD values are interpreted as strike-slip faults. This approach has proven effective in various recent studies for distinguishing fault types in tectonically complex regions [3],[9].

The initial density values used in the forward modeling were determined based on regional geological information and typical density ranges of sedimentary and volcanic rocks. These values served as initial model parameters and were subsequently refined through an iterative forward modeling process until an acceptable fit between observed and calculated gravity anomalies was achieved. The final stage of data processing was two-dimensional (2D) forward modeling, which aimed to validate the interpreted geological structures. This modeling was carried out using Oasis Montaj software, which is widely used in gravity data analysis. The subsurface model was constructed based on the fit between the model response and the observed anomaly data, resulting in a geological representation that closely approximates the actual subsurface conditions [4].Thus, the integration of spectral analysis, FHD, SVD, and 2D modeling provides a comprehensive approach for identifying and validating subsurface fault structures in the study area [25].

3. Results and Discussion

The Complete Bouguer Anomaly (CBA) map represents the distribution of gravity anomalies that have undergone a series of corrections and reflect variations in subsurface rock density caused by both regional and local geological heterogeneity [28–29].

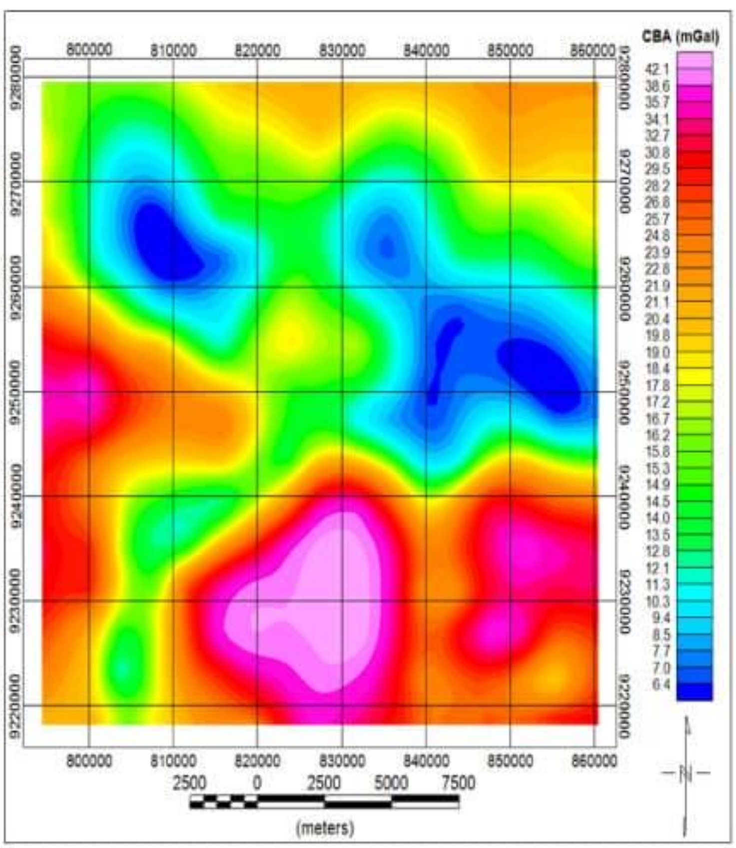

Figure 4. Complete Bouguer Anomaly (CBA) Map of the Sumedang Region

Variations in anomaly values on the CBA map are influenced by differences in rock mass density, making the gravity method highly effective for identifying geological structures such as faults, folds, basins, and igneous intrusions. The information contained in the CBA map still includes regional, residual, and noise components. Therefore, filtering processes are required to improve the quality of subsurface interpretation [16].

The CBA map shown in Figure 4 presents anomaly values ranging from 6.4 to 42.1 mGal, with high anomalies dominating the southern part of the study area, while low anomalies dominate the northern part. This anomaly pattern indicates the presence of rock density contrasts associated with geological structures and regional tectonic activity in West Java [1].

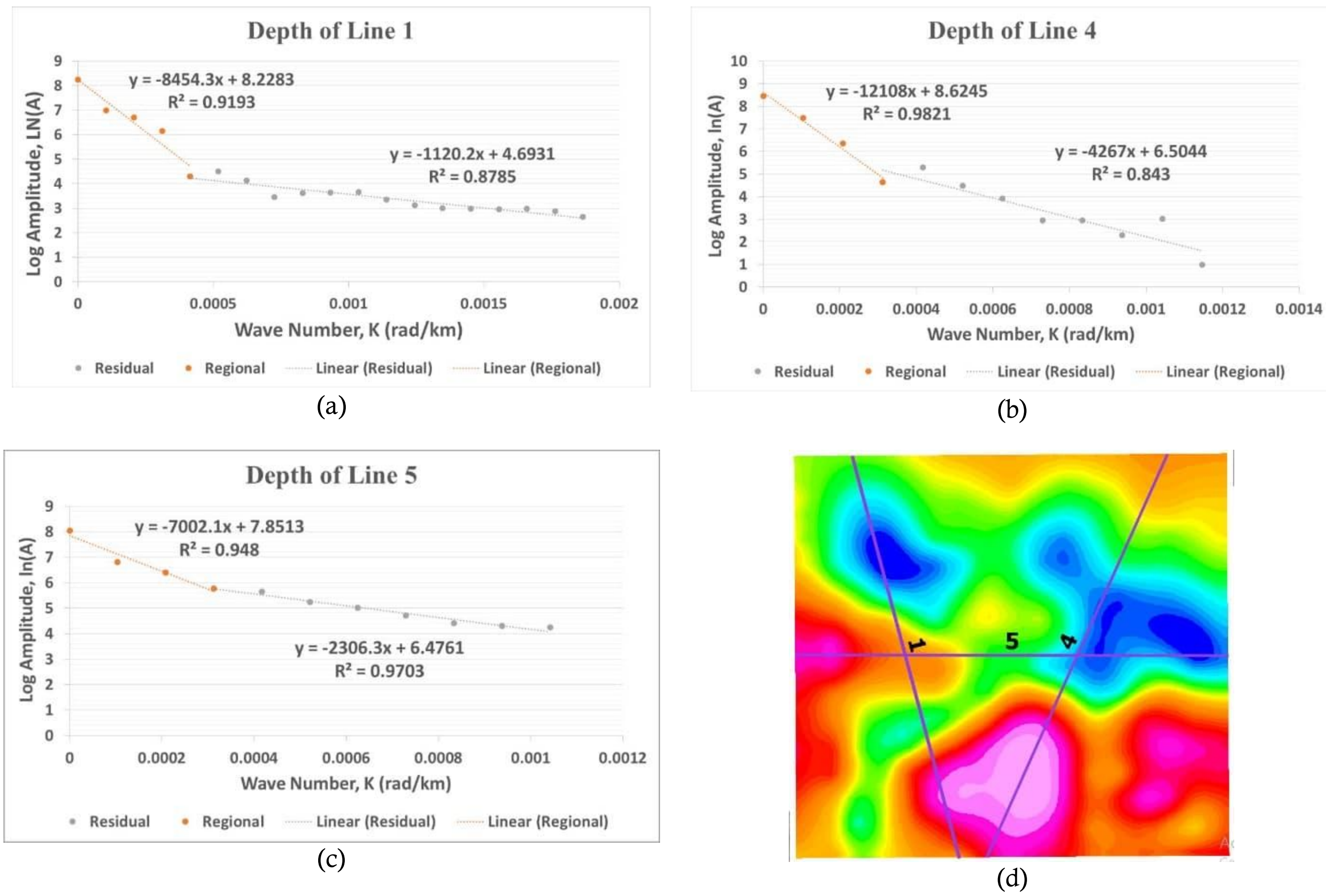

Figure 5. Regional and Residual Depth Analysis: (a) Line 1, (b) Line 4, (c) Line 5, and (d) profile lines on the CBA map

Depth analysis of anomaly sources was carried out using the spectral analysis method on CBA data that had been separated along specific profiles. The Fourier spectral method was used because it is capable of separating low-frequency and high-frequency components, making it effective for estimating the depths of regional and residual anomaly sources. In this study, three profile lines were used, namely lines 1 and 4 trending north–south and line 5 trending west–east. Fourier transformation of the gravity anomaly data produced a relationship between the wave number (wavenumber, k) and amplitude (Ln A), which was subsequently used to determine the cutoff value based on the intersection of two spectral gradient segments [30–31]. This method is commonly used to separate shallow and deep anomaly sources in regional gravity studies [32–33].

The spectral analysis results in Table 2 indicate an average regional depth of 9188.13 meters and an average residual depth of 2564.5 meters. The regional depth represents deep anomaly sources such as the basement or crustal structures, whereas the residual depth indicates the presence of shallow sources such as faults, fractures, and local lithological boundaries [34]. Interpretation of the gradient on the spectral curves allows quantitative estimation of anomaly source depths and has been widely applied in studies of active tectonics and geothermal exploration [4].

Table 2. Depths Obtained from Spectral Analysis

Line	Regional Depth (m)	Residual Depth (m)
1	8454.3	1120.2
2	12108	4267
3	7002.1	2306.3
Average	9188.13	2564.5

The separation of regional and residual anomalies was performed using a Gaussian filter to enhance the resolution of shallow anomalies and reduce the influence of regional fields originating from deeper sources [16]. The regional anomaly map shown in Figure 6 has anomaly values ranging from 6.5 to 41.9 mGal and represents regional geological responses such as the basement and large-scale tectonic structures [1]. High anomaly values are interpreted to be associated with high-density rocks such as volcanic rocks or intrusive bodies, whereas low anomalies are associated with low-density sediments [11].

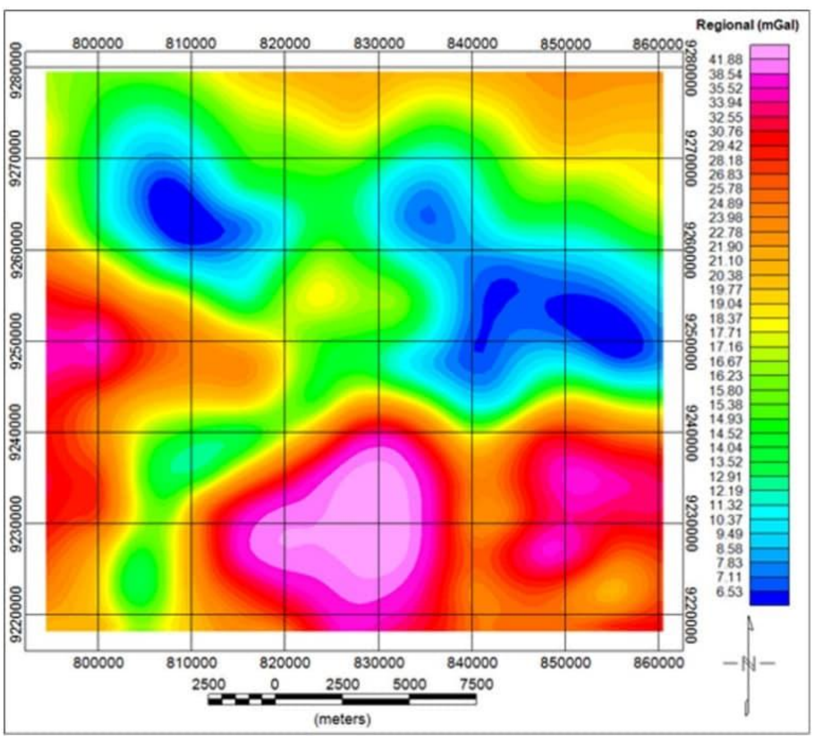

Figure 6. Regional Anomaly Map of the Sumedang Region

Meanwhile, the residual anomaly map shown in Figure 7 has anomaly values ranging from -6.1 to 7.4 mGal and displays more detailed anomaly variations. Residual anomalies are highly sensitive to shallow structures such as faults, lithological contacts, fractures, and alteration zones because the influence of deeper sources has been minimized through the filtering process [15–16]. Density contrast variations on the residual anomaly map indicate the presence of subsurface geological deformation associated with active tectonic activity in the Sumedang region [7][22–23][35–37].

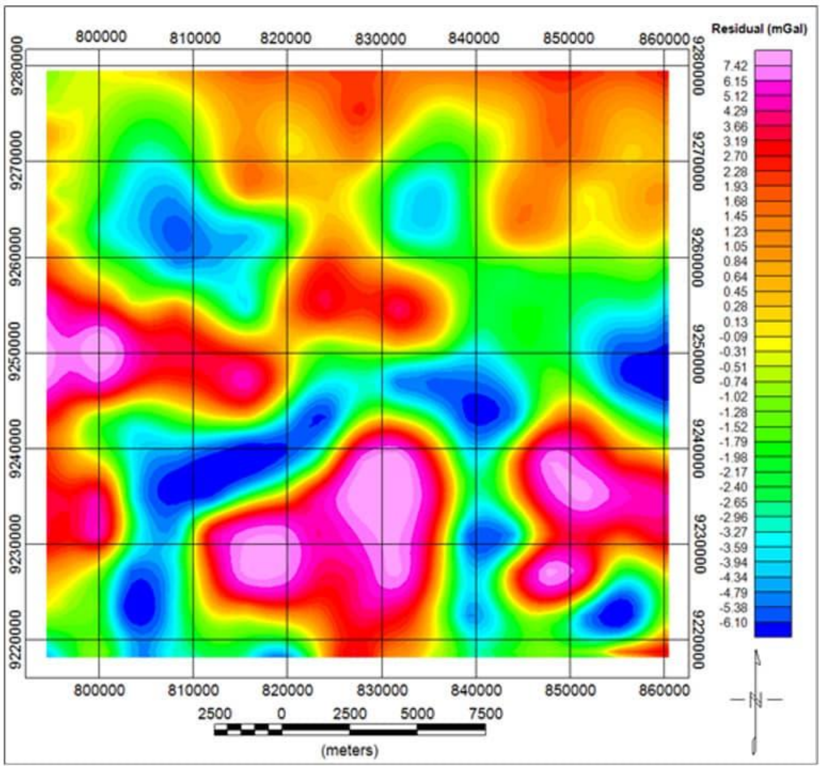

Figure 7. Residual Anomaly Map of the Sumedang Region

Gravity anomaly derivative analysis was carried out using the First Horizontal Derivative (FHD) and Second Vertical Derivative (SVD) methods. The FHD method is effective for identifying lateral anomaly boundaries and highlighting maximum gradient zones associated with fault planes or lithological contacts. On the FHD map shown in Figure 8, high values are represented by pink to orange color gradations, indicating the presence of high density contrasts caused by fault structures or significant lithological changes [3]. In contrast, low values shown in blue represent relatively homogeneous zones with weak density gradients.

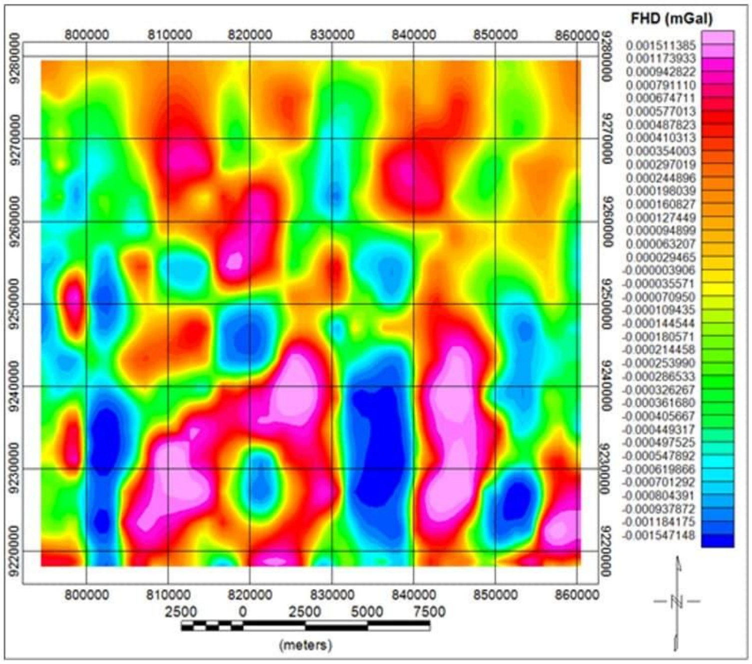

Figure 8. First Horizontal Derivative (FHD) Map of the Sumedang Region

The SVD method shown in Figure 9 was used to enhance shallow anomaly responses through the second derivative in the vertical direction, thereby improving the resolution of subsurface structures [15]. High positive values indicate density changes from low to high, whereas negative values indicate the opposite density contrast [15]. SVD is highly sensitive to noise but has a strong capability for detecting geological structure boundaries and active faults [3][38]. Therefore, the integration of FHD and SVD provides more reliable interpretations compared to the use of a single method [9].

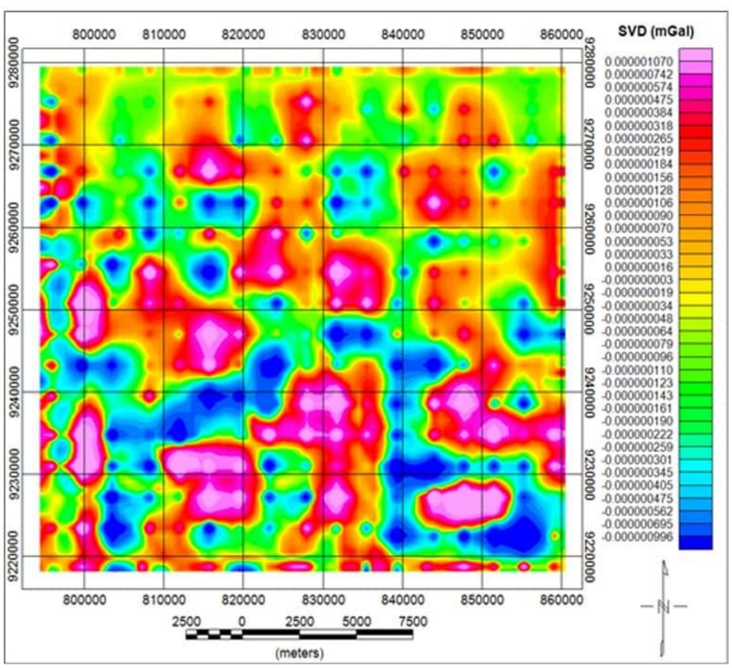

Figure 9. Second Vertical Derivative (SVD) Map of the Sumedang Region

A total of seven profile lines were extracted from the residual anomaly map and used for 2D forward modeling using Oasis Montaj software. The profile lines were determined based on anomaly contrasts and the presence of active Java–Bali–NTB faults. The integration of residual, FHD, and SVD data along each profile enabled more accurate fault identification because the SVD zero points generally coincide with the extreme values of the FHD in zones of high-density contrast. The correlation among these three curves indicates that fault structures developed within zones characterized by sharp gradients in the residual anomaly [3],[34].

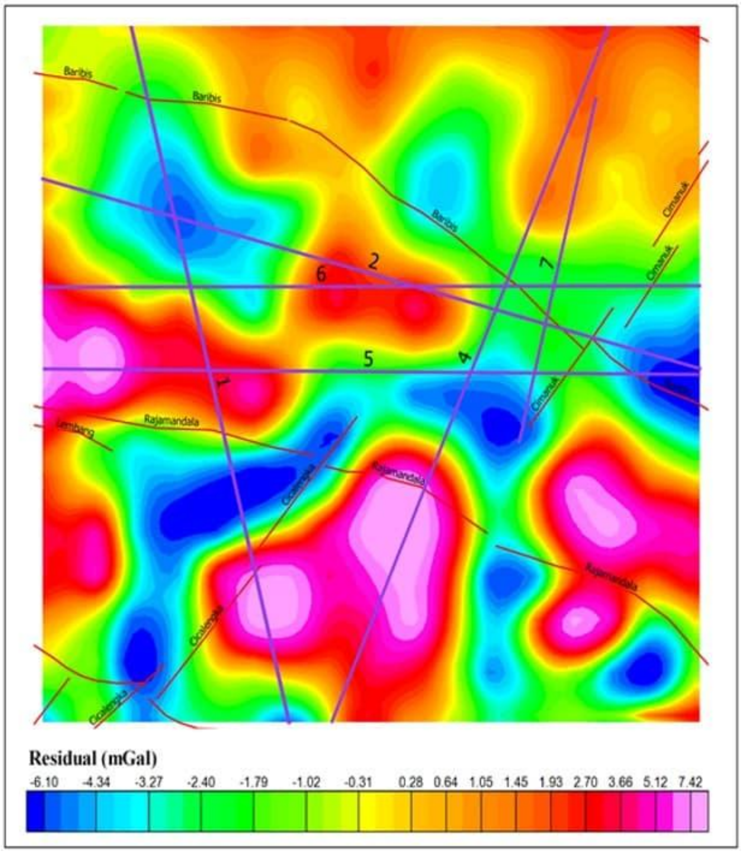

Figure 10. Determination of profile lines used for residual anomaly modeling

In addition, the same seven profiles were extracted from the FHD and SVD anomaly maps using Surfer v.29 software. The resulting profiles were then used to examine the correlation between the residual, FHD, and SVD curves. The profile graphs demonstrate the relationship among the curves, where fault locations are identified at the SVD zero points that coincide with the extreme values of the FHD and are supported by contrasts in the residual curve. Fault locations can be identified based on the FHD graph, whereas fault types can be interpreted from the SVD graph. The fault orientation was determined from the SVD response pattern to rock density contrasts, further strengthening the interpretation of fault plane positions.

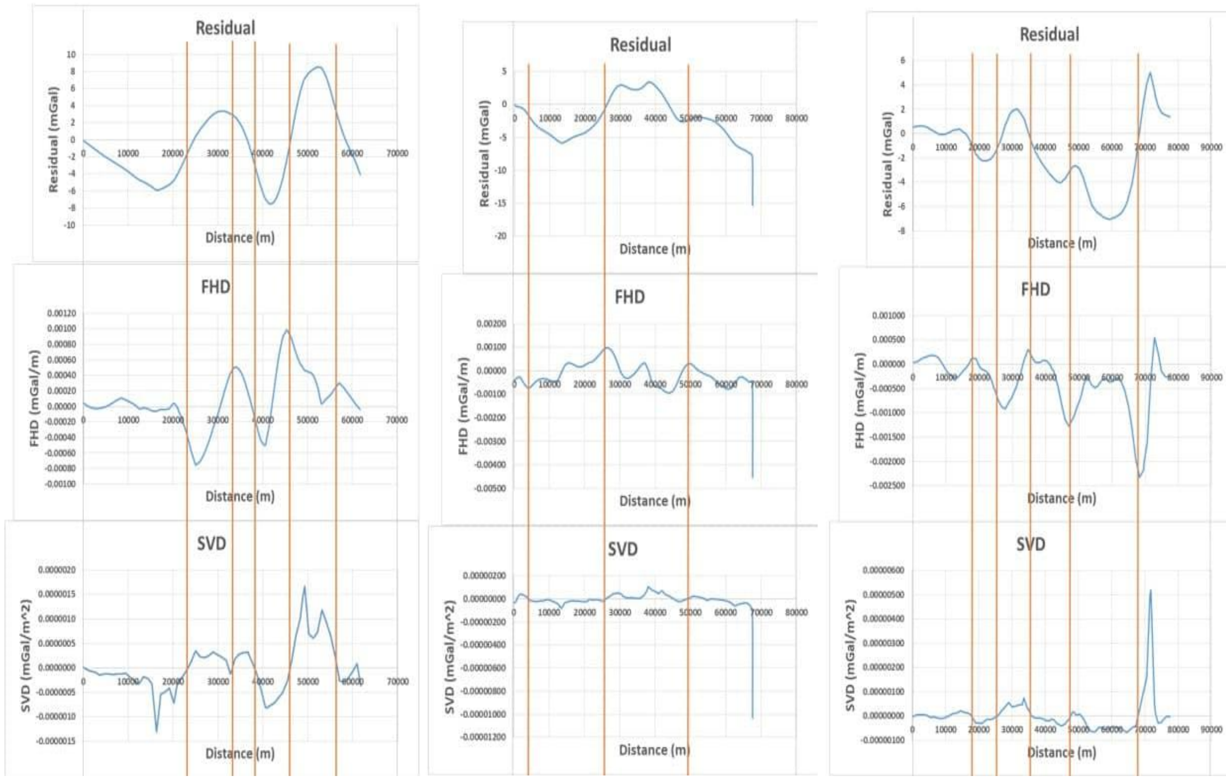

A B C

Figure 11. Correlation graphs of residual anomaly, FHD, and SVD: (A) Line 1, (B) Line 2, and (C) Line 3

Based on Figure 11(A), line 1 indicates the presence of five fault structures consisting of reverse and normal faults. One fault on the first line has an |SVD MAX| value of 0.00000035 mGal/m² and an |SVD MIN| value of -0.000000717 mGal/m². Fault type interpretation was conducted based on the relationship between the |SVD MAX| and |SVD MIN| values, where reverse faults are characterized by |SVD MAX| < |SVD MIN|, while normal faults show the opposite condition. On line 1, which trends northwest–southeast, the more dominant |SVD MIN| value located on the left side indicates that the fault tendency is directed toward the southeast. This pattern suggests the simultaneous occurrence of compressional and extensional deformation within the study area [1]. On line 5, the presence of a strike-slip fault with reverse components was interpreted based on the relatively similar maximum and minimum SVD values, indicating dominant horizontal movement with a minor vertical component [4],[7]. The summary of fault analysis results for lines 1 to 3 shows that the maximum and minimum SVD values obtained from each profile can be used to identify fault characteristics and orientations (Table 3).

Table 3. Fault Analysis Results for Lines 1 to 3

Line	Distance (m)	Minimum SVD (mGal/m²)	Maximum SVD (mGal/m²)	Fault Characteristics	Fault Direction
1	23090.91	-0.000000717	0.00000035	Reverse Fault	Southeast
1	32944.15	-0.000000126	0.000000323	Normal Fault	Northwest
1	38616.72	-0.000000810	0.000000323	Reverse Fault	Northwest
1	46379.62	-0.000000810	0.000001661	Normal Fault	Northwest
1	56892.05	-0.000000290	0.000001179	Normal Fault	Southeast
2	4635.506178	-0.00000022	0.00000040	Normal Fault	East
2	26247.60847	-0.00000018	0.00000050	Normal Fault	West
2	49824.44733	-0.00000023	0.00000025	Normal Fault	West
3	17861.88269	-0.00000030	0.00000012	Reverse Fault	Northeast
3	25711.84219	-0.00000016	0.00000057	Normal Fault	Northeast
3	35804.64726	-0.00000009	0.00000073	Normal Fault	Southwest
3	47018.87511	-0.000000404	0.00000017	Reverse Fault	Southwest
3	67958.8945	-0.00000044	0.00000162	Normal Fault	Northeast

In Figure 12(C), line 5, the third fault line shows an |SVD MAX| value of 0.00000013 mGal/m² and an |SVD MIN| value of -0.00000020 mGal/m², which are relatively similar. These values indicate a relatively low anomaly contrast, suggesting only minor differences in rock density on both sides of the fault. This condition is generally associated with the characteristics of strike-slip faults dominated by horizontal movement. However, the slight difference between the maximum and minimum values also indicates the presence of a vertical component. Therefore, the fault along this profile is interpreted as a strike-slip fault with reverse components. The results of the fault analysis for lines 4 to 7 are presented in Table 4.

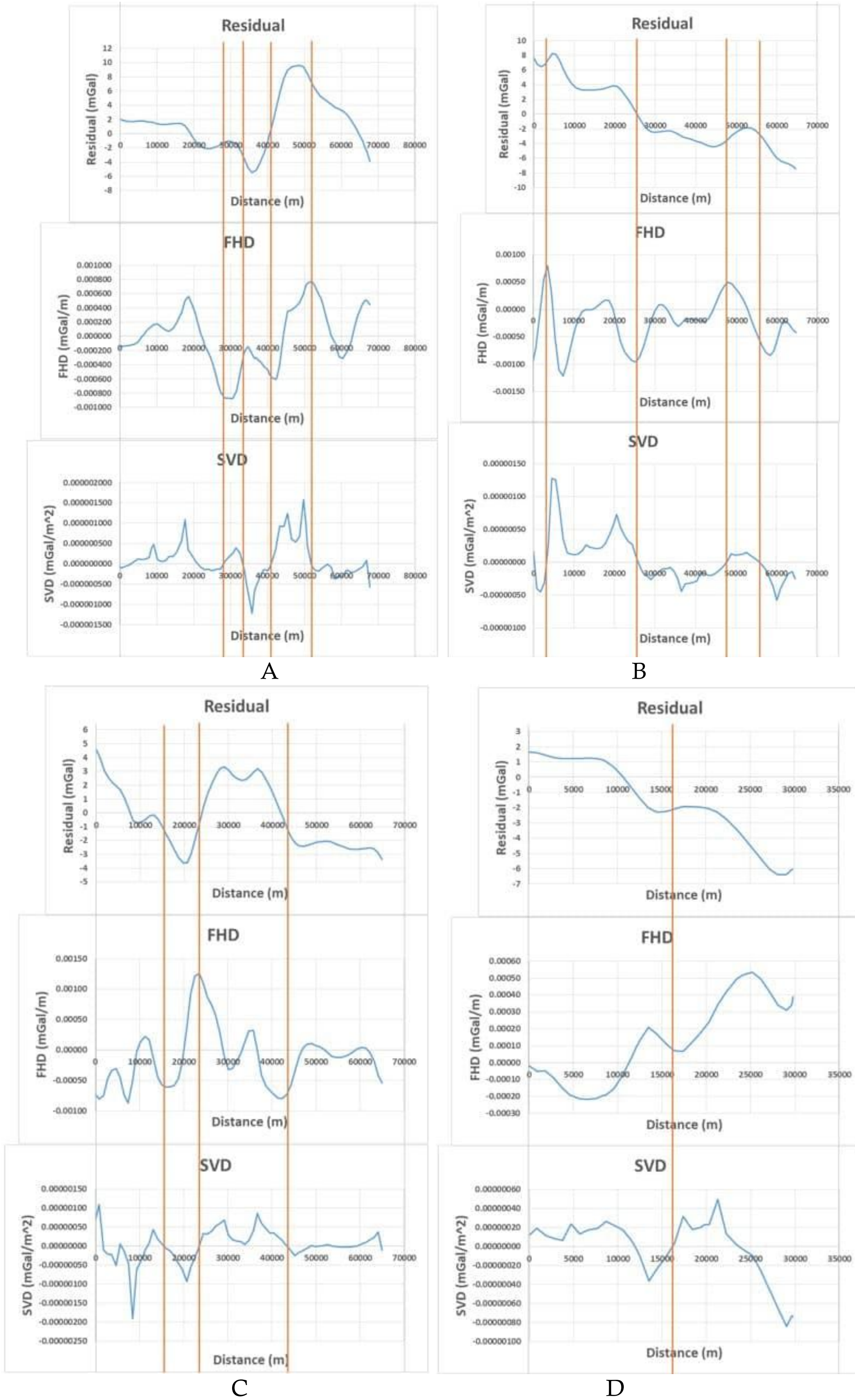

Figure 12. Correlation graphs of residual anomaly, FHD, and SVD: (A) Line 4, (B) Line 5, (C) Line 6, and (D) Line 7

Table 4. Fault Analysis Results for Lines 4 to 7

Line	Distance (m)	Minimum SVD (mGal)	Maximum SVD (mGal)	Fault Characteristics	Fault Direction
4	28346.82481	-0.000000135	0.000000396	Normal Fault	Northeast
4	33696.98606	-0.0000012141	0.0000003957	Reverse Fault	Northeast
4	40482.78829	-0.000000160	0.000000933	Normal Fault	Northeast
4	51887.5343	-0.000000177	0.000001574	Normal Fault	Southwest
5	3597.202353	-0.00000045	0.00000125	Normal Fault	West
5	25283.88151	-0.00000017	0.00000028	Normal Fault	East
5	47913.45977	-0.00000020	0.00000013	Strike-Slip Fault	East
5	56399.55161	-0.00000058	0.00000015	Reverse Fault	West
6	15949.68725	-0.00000013	0.00000018	Normal Fault	East
6	23492.88411	-0.00000055	0.00000033	Reverse Fault	East
6	43293.77587	-0.00000025	0.00000035	Normal Fault	East
7	15914.28	-0.00000023	0.00000004	Reverse Fault	Southwest

The fault analysis results for lines 1 to 7 presented in Tables 3 and 4 were used as references for the 2D forward modeling. The modeling was carried out using the GM-SYS filter through a forward modeling approach by utilizing residual gravity anomalies to confirm subsurface geological structures. The model was constructed using the residual depth of -2564.5 meters as the shallow layer and the regional depth of -9188.13 meters as the basement boundary. The forward modeling approach was applied to estimate subsurface geometry based on the gravity anomaly response [30–31]. The stratigraphic model was divided into three main units, namely younger sediment, older sediment, and basement [32], as shown in Figures 13 to 19.

Based on the modeling results, line 1 (Figure 13), which trends northwest–southeast, indicates the presence of five fault structures consisting of two reverse faults and three normal faults. The reverse faults are interpreted to dip toward the southeast and northwest, characterized by sharp residual anomaly gradients and FHD and SVD responses that show significant density contrast changes caused by active fault deformation [3][15]. Meanwhile, line 2 (Figure 14), which extends west–east, is dominated by three normal faults, indicating an extensional regime. Line 3 (Figure 15) shows a combination of two reverse faults and three normal faults. However, the interpretation along this line has higher uncertainty due to the relatively weak anomaly contrasts. Therefore, line 3 was not used as the primary reference for correlation with regional active fault structures.

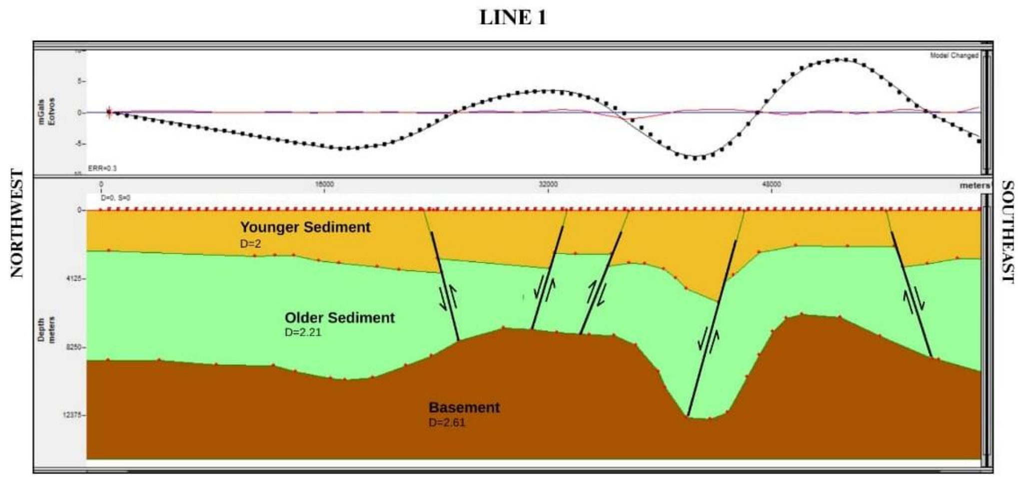

Figure 13. Residual anomaly cross-section of Line 1

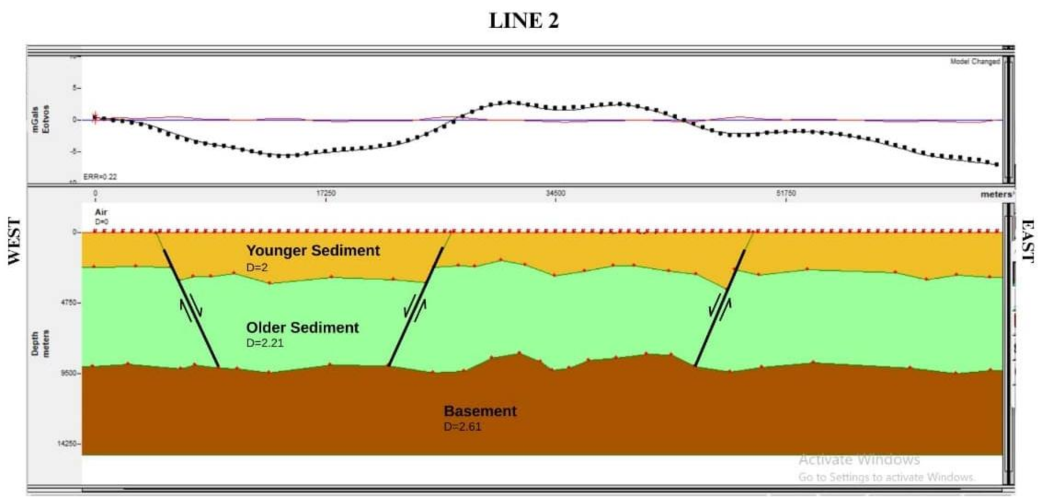

Figure 14. Residual anomaly cross-section of Line 2

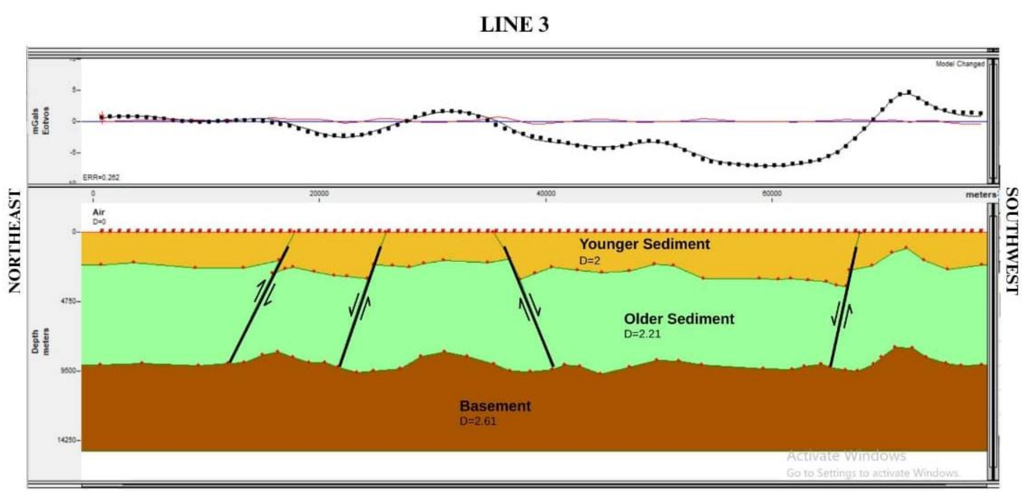

Figure 15. Residual anomaly cross-section of Line 3

LINE 4

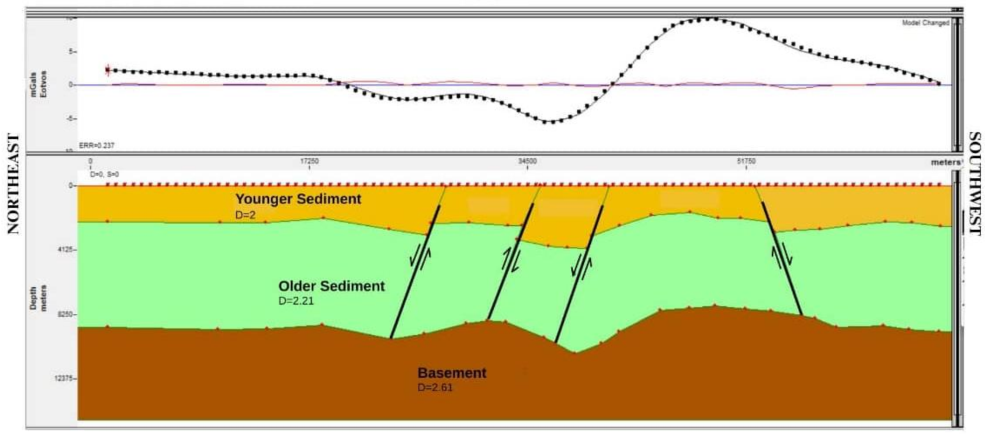

Figure 16. Residual anomaly cross-section of Line 4

LINE 5

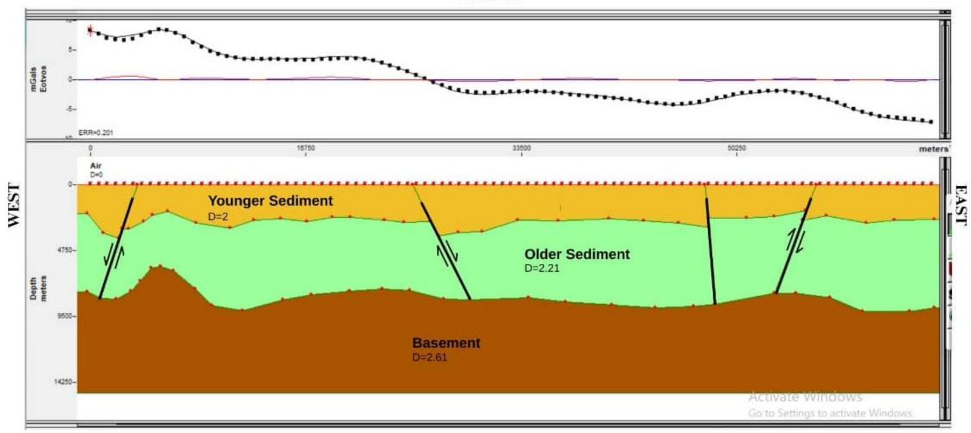

Figure 17. Residual anomaly cross-section of Line 5

LINE 6

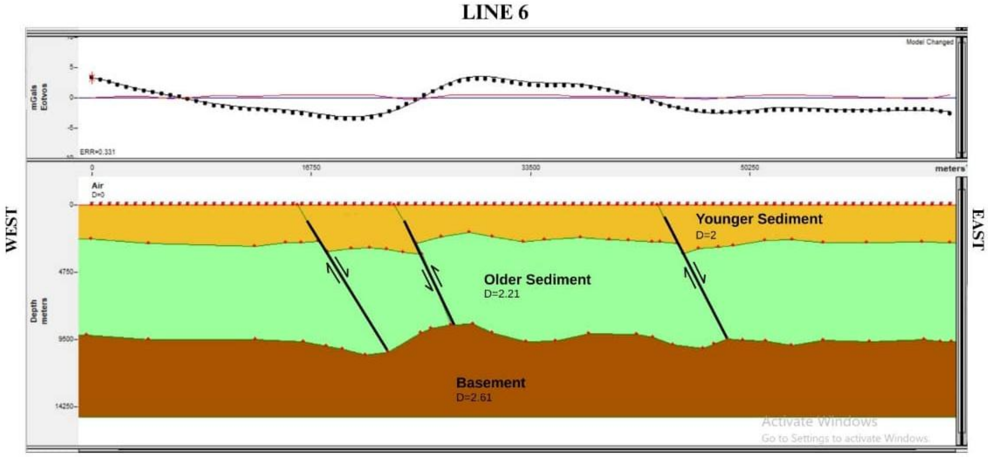

Figure 18. Residual anomaly cross-section of Line 6

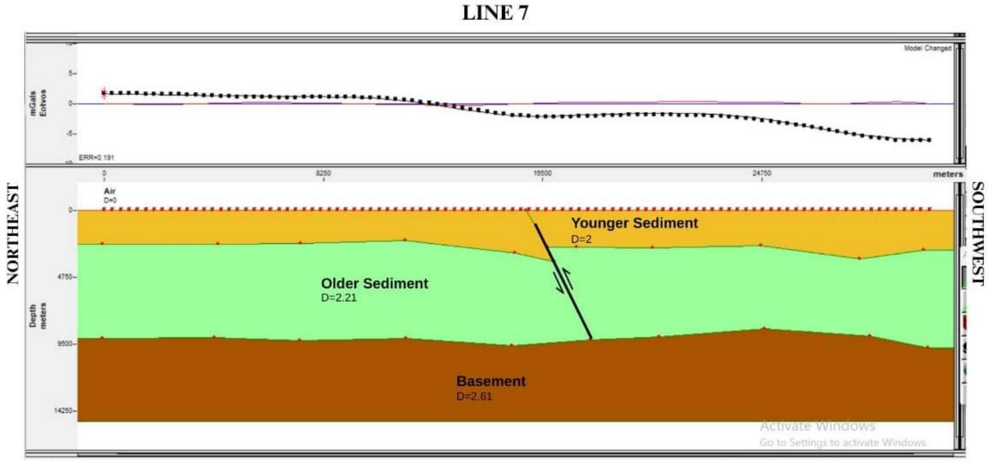

Figure 19. Residual anomaly cross-section of Line 7

Lines 4 (Figure 16) and 5 (Figure 17) again indicate the presence of reverse and normal faults, with an additional strike-slip fault with reverse components identified on line 5, suggesting the presence of oblique-slip movement resulting from a combination of compressional and shear forces [11]. Line 6 (Figure 18) is dominated by normal faults with one reverse fault, whereas line 7 (Figure 19) shows only one reverse fault with a relatively weak anomaly response. Overall, the presence of fault structures along each profile correlates with changes in residual anomaly gradients as well as FHD and SVD derivative patterns, indicating density contrast boundaries between rock units at shallow to intermediate depths.

Based on the Java–Bali–NTB active fault database, the Sumedang region is crossed by the Baribis Fault, Cimanuk Fault, Rajamandala Fault, and Cicalengka Fault. The presence of these faults is closely related to regional tectonic activity resulting from the subduction of the Indo-Australian Plate beneath the Eurasian Plate [1]. The interpretation results indicate that the Baribis Fault was identified as a reverse fault on lines 5 and 7, whereas the Cimanuk Fault was identified as a strike-slip fault with reverse components on line 5 [7][35–37]. Validation against active fault data shows that the gravity interpretation results are consistent with the regional geological conditions of West Java [1]. The Rajamandala Fault is interpreted as a reverse fault observed on line 1, based on the integration of residual anomaly, FHD, SVD, and 2D forward modeling results.

The fault interpretation results generally show good agreement with the spatial distribution of major faults contained in the Java–Bali–NTB active fault database. However, several interpreted structures do not directly coincide with the mapped fault traces. This discrepancy may be related to differences in spatial resolution between gravity-derived interpretations and surface geological mapping, as well as the influence of subsurface density contrasts that are not always expressed at the surface. In addition, gravity data represent an integrated response of subsurface mass distribution, resulting in a degree of uncertainty in determining the exact position and geometry of fault structures. Nevertheless, the consistency observed between several interpreted faults and the regional fault framework supports the reliability of the interpretation results.

The identified fault structures are also supported by regional tectonic and seismic studies in West Java, which indicate ongoing crustal deformation and shallow seismic activity associated with active fault systems [35–37]. The correspondence between the interpreted fault locations and the active fault database suggests that the detected structures remain tectonically significant and continue to influence geological processes in the Sumedang area. These results demonstrate that the integration of FHD, SVD, and 2D forward modeling is capable of delineating major subsurface fault structures and provides a reliable approach for structural interpretation in tectonically complex regions. Validation of the fault analysis results in this study using the Java–Bali–NTB active fault database is presented in Figure 20.

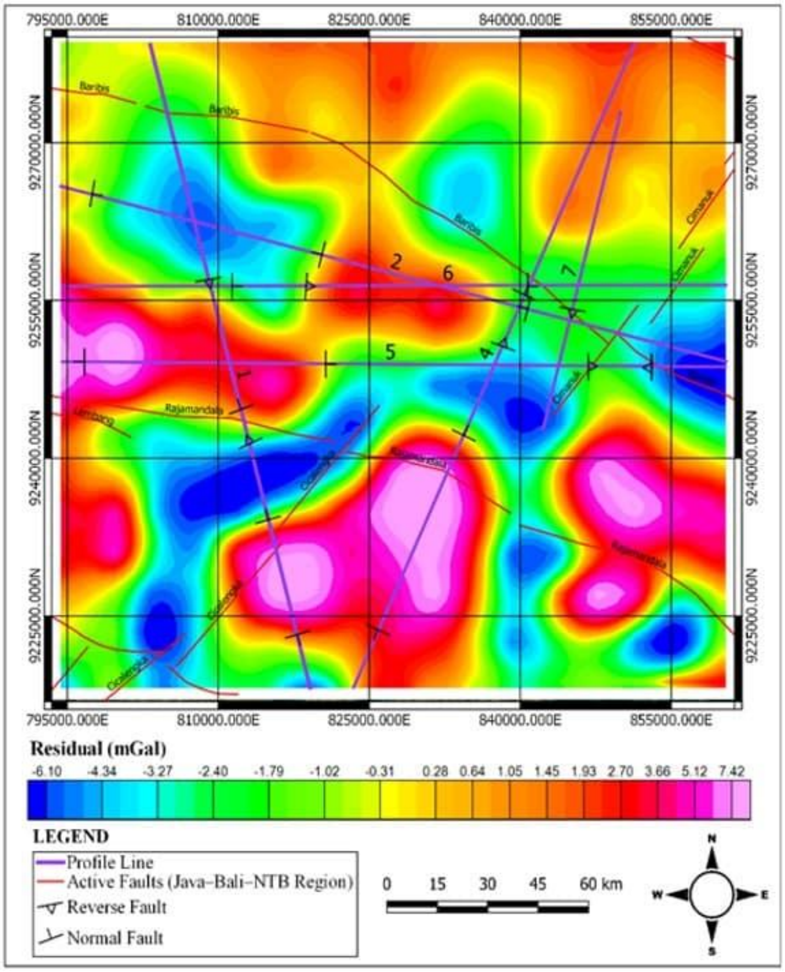

Figure 20. Map of Fault Identification Results in the Sumedang Region Based on the Residual Anomaly Map

The presence of reverse faults, normal faults, and strike-slip faults within the same region indicates that the study area is affected by a complex tectonic regime resulting from a combination of compressional, transtensional, and transpressional deformation [11]. This deformation system has developed dynamically within the active tectonic zone of Java, which continues to be influenced by ongoing subduction activity. Therefore, the results of this study not only identify subsurface structures using the gravity method but also provide important information for mitigating geological hazards such as earthquakes and landslides in the Sumedang region.

4. Conclusion

The identification of fault structures based on gravity data through residual anomaly, First Horizontal Derivative (FHD), and Second Vertical Derivative (SVD) analysis revealed the presence of several fault structures in the Sumedang region with varying types and orientations following the directions of the measurement lines. Structural interpretation was carried out through the correlation between the residual curves, the extreme values of the FHD, and the zero points on the SVD curves that coincide with the maximum and minimum FHD values, allowing subsurface structural boundaries to be identified more clearly. Fault types were determined based on the relationship between the |SVD MAX| and |SVD MIN| values, where reverse faults are characterized by |SVD MAX| < |SVD MIN|, whereas normal faults show the opposite condition. In addition, the fault tendency direction was determined based on the dominant position of the |SVD MAX| or |SVD MIN| values relative to the orientation of the measurement lines.

Based on correlations with the Java–Bali–West Nusa Tenggara active fault database, several identified structures are associated with major regional faults in the study area. The Baribis Fault was interpreted as a reverse fault on lines 5 and 7, the Rajamandala Fault was interpreted as a reverse fault on line 1, whereas the Cimanuk Fault exhibits the characteristics of a strike-slip fault with reverse components on line 5. These interpretation results indicate that the Sumedang region is influenced by compressional, extensional, and strike-slip deformation that developed complexly in accordance with the regional tectonic setting of West Java.

Therefore, the gravity method through FHD and SVD analysis has proven to be effective in identifying subsurface fault structures and describing geological deformation patterns in the Sumedang region. The integration of residual, FHD, and SVD analysis provides more detailed information regarding the type, orientation, and tendency of fault structures.

References

[1] Aribowo, S., Husson, L., Natawidjaja, D. H., Authemayou, C., Daryono, M. R., Puji, A. R., ... & Lorcery, M. (2022). Active back-arc thrust in north west Java, Indonesia. *Tectonics,* 41(7), e2021TC007120.

[2] Wandono, W., Ramdhan, M., Aulia, A. N., Pangestu, A. B., Hidayat, E., Syuhada, S., ... & Maulana, M. P. (2025). Seismic velocity structure beneath the western Java region, Indonesia, from local earthquake tomography. *Journal of Volcanology and Geothermal Research,* 108472.

[3] Hofi, L. N., Maryanto, S., Susilo, A., & Wuryani, S. D. (2024). Derivative analysis of gravity data in revealing subsurface fault structure model in Semeru Volcano, East Java and its surrounding. *Trends in Sciences, 21*(9), 8050.

[4] Heliani, L. S., Pratama, C., Anggraini, A., Dewanto, B. G., Natul, A. S., & Lestari, D. (2025). Integrated gravity, GNSS, and seismic analysis for fault mapping in Sulawesi Island: Insights into the Palu-Koro Fault. *Geodesy and Geodynamics, 16*(2), 145–158.

[5] Purwaningsih, R. E. Y., Sekarsari, A., Sari, T. W., Pratama, C., & Wibowo, S. T. (2022). Active tectonics of the eastern java based on a decade of recent continuous geodetic observation. *Geodesy and Geodynamics,* 13(4), 376-385.

[6] Arisbaya, I., Wijanarko, E., Warsa, Sumintadireja, P., Sudrajat, Y., Handayani, L., ... & Grandis, H. (2023). Magnetotellurics (MT) and gravity study of a possible active fault in Southern Garut, West Java, Indonesia. *International Journal of Geophysics,* 2023(1), 4482074.

[7] Saputra, S. E. A., Wahyudi, J., & Budianto, A. (2024). *Gempa bumi Sumedang 31 Desember 2023*. Bandung: Kementerian Energi dan Sumber Daya Mineral.

[8] Syafarudin, I. (2025). Investigasi karakteristik bawah permukaan di sekitar sumber gempa Sumedang 31 Desember 2023 menggunakan parameter Vs30 dan kurva HVSR guna pemetaan daerah rawan potensi gempa. *Jurnal Geofisika, 22*(2), 22–26.

[9] Permana, N. R., Fadrian, D. F., Gunawan, B., & Wulandari, A. (2024). Distribution of geological structures on Java Island based on derivative analysis of satellite gravity data. *Jurnal Penelitian Fisika dan Aplikasinya, 14*(2), 154–168.

[10] Mazzaluna, H. P., & Wibowo, R. C. (2024). Geological Structure Identification Using GGMplus Satellite Gravity Data in The Area Surrounding Mount Tampomas. *EKSPLORIUM*, 45(1), 27-38.

[11] Restiana, A., Zani, F. R., & Wardhianty, N. F. (2023, December). Identification of Geothermal System Structure Based on Derivative Analysis and 3D Model of Gravity Satellite Data of Mount Rajabasa Area, South Lampung. In *IOP Conference Series: Earth and Environmental Science* (Vol. 1288, No. 1, p. 012014). IOP Publishing.

[12] Lumbantoruan, I. N., Sarkowi, M., Mulyatno, B. S., & Wibowo, R. C. (2023). Identifikasi Struktur Patahan Dan Lokasi Reservoar Panasbumi Daerah Gunung Ciremai Berdasarkan Analisis Data Gravity. *Jurnal Geosaintek,* 9(2), 70-79.

[13] Eshaghzadeh, A., & Hajian, A. (2022). Modelling of residual gravity data due to a near surface dyke structure using damped SVD and marquardt inverse methods. *Geofisica internacional,* 61(4), 325-350.

[14] Pascaning Setiahadiwibowo, A., Setiawan, A., Husein, S., & Sismanto, S. (2025). Subsurface Structural Modelling using the Gravity Method in the Pacitan Area, Indonesia based on Derivative Analysis and Model Inversion. *Rudarsko-geološko-naftni zbornik,* 40(1), 51-61.

[15] Rinanda, S. T. (2024). Identification of the subsurface structure of the Great Sumatra Fault Dikit Segment based on first horizontal derivative (FHD), second vertical derivative (SVD), and forward modelling analyses of 2D gravity anomaly data. *Jurnal Geofisika, 22*(2), 13–21.

[16] Karunianto, A. J., Haryanto, D., Hikmatullah, F., & Laesanpura, A. (2017). Penentuan anomali gayaberat regional dan residual menggunakan filter Gaussian Daerah Mamuju Sulawesi Barat. *Eksplorium*, 38(2), 89-98.

[17] Jayatri, A. U., Multi, W., & Hayatuzzahra, S. (2023). Identifikasi Keberadaan Sesar Menggunakan Metode Gravitasi dan Analisis Second Vertical Derivative (SVD) di Bagian Selatan Kabupaten Sumbawa. *Jurnal Tambora,* 7(2), 53-57.

[18] Yusvinda, M. N., Puspitasari, S. W., Wafi, N. M., Aziz, K. N., Darmawan, D., Katriani, L., ... & Wibowo, N. B. (2021, March). Structure Interpretation Using Gravity Spectral Analysis and Derivative Method in Grindulu Fault, Pacitan, East Java. In *7th International Conference on Research, Implementation, and Education of Mathematics and Sciences* (ICRIEMS 2020) (pp. 415-420). Atlantis Press.

[19] Nurhasan, R., MN, H., Setiawan, A., Gumelar, F., Fitriani, D., Sutarno, D., ... & Rusdiana, R. (2023). Identification of geological structure based on gravity method in Tangkuban Parahu Volcano, Bandung, Indonesia. *IOP Conference Series Earth and Environmental Science.*

[20] Zulkaromi, M., Setiadi, I., Suharno, S., Mulyatno, B. S., Haerudin, N., & Ferucha, I. (2021). Identification of Horst and Graben Structural Patterns Using Gravity and Second Vertical Derivative (SVD) Methods in The Lubuksikaping Area of West Sumatera. *Indonesian Physical Review,* 4(3), 153-165.

[21] Safira, A., Saipuddin, M., Andita, Z, A. (2024). Identifikasi Struktur Geologi Daerah Panas Bumi Way Panas Kecamatan Wonosobo Menggunakan Analisis First Horizontal Derivative dan Second Vertical Derivative Berdasarkan data Gaya Berat GGMPLUS. *Jurnal Pendidikan, Sains, Geologi, dan Geofisika (GeoScienceEd),* 5(1), 28-35.

[22] Rasimeng, S., Pratama, T. P. E., & Wibowo, R. C. (2024). Structural Geology Identification based on Derivative Analysis Gravity Data in Tangkuban Perahu Mountain. *Journal of Engineering and Scientific Research,* 6(1), 7-15.

[23] Wibowo, R. C., Tobing, J. B. L., & Alimudin, A. (2022). Geological Structure Identification using Derivative Analysis of Gravity Method. *Journal of Innovation and Technology,* 3(2), 30-36

[24] Ananda, R., Azhari, N. I. Y., Rahadinata, T., & Grandis, H. (2026). Analysis of Gravity Data for Basement Depth Estimation of the Western Part of Java Island, Indonesia. *Journal of Engineering and Technological Sciences,* 58(1), 1-16.

[25] Hanif, M., Handayani, L., Arisbaya, I., Aulia, A. N., & Gaol, K. L. (2021). Analysis of gravity anomaly decomposition and depth to basement, case study: Cenozoic Bogor Basin, Indonesia. *Journal of Geoscience, Engineering, Environment, and Technology,* 6(1), 51-57.

[26] Fitriani, D. S., Putri, S. N. A., & Putrajy, I. F. (2020). Metode gravitasi untuk identifikasi sesar Weluki dengan analisis first horizontal derivative dan second vertical derivative. *Prosiding Seminar Nasional Fisika* (pp. SNF2020FA-53–SNF2020FA-60). Jakarta: Universitas Negeri Jakarta.

[27] Sumintadireja, P., Dahrin, D., & Grandis, H. (2018). A note on the use of the second vertical derivative (SVD) of gravity data with reference to Indonesian cases. *Journal of Engineering and Technological Sciences, 50*(1), 127–139.

[28] Sarkowi, M., Yusuf, M., & Minardi, S. (2023). Identifikasi struktur Iliran High Sumatera Selatan berdasarkan analisa anomali gravity. *JGE (Jurnal Geofisika Eksplorasi), 9*(2), 150–160.

[29] Alhassan, A., & Aliyu, A. (2022). The Principle of Interpretation of Gravity Data Using Second. *Gravitational Field: Concepts and Applications,* 143.

[30] Handayani, A. T., Adhi, M. A., & Nurcahya, B. E. (2025). 2D Modeling of Subsurface Structures Based on Gravity Data of Mount Arjuno-Welirang. *Physics Education Research Journal,* 7(2), 49-54.

[31] Althafunnisa, N. A., Herbianto, S. A., & Setyawan, A. (2024). Applications of Gravity Method Based on Satellite Image Anomaly Data to Identify Subsurface Structures. *Journal of Physics and Its Applications*, 6(2), 61-67.

[32] Li, S., Zhang, S., Ga-La-Tu, J. R., & Dai, X. (2025). Investigating the gravity variable-density inversion method in complex geological settings: Application to the South China Sea. *Journal of Geophysics and Engineering, 22*(6), 1700–1709.

[33] Zhou, W., Sun, Y., Zhang, W., Yao, G., & Wu, R. (2025). Interpretation of gravity-seismic joint inversion and its application in Longmenshan region. *Geosystems and Geoenvironment*, 100469.

[34] Apeh, O. I., Pham, L. T., Prasad, K. N. D., Tenzer, R., & Moka, E. C. (2024). Gravity-based structural mapping of the southern Benue Trough, Nigeria. *Environmental Earth Sciences,* 83(24), 685.

[35] Daryono, M. R., Natawidjaja, D. H., Puji, A. R., & Aribowo, S. (2021, October). Fault rupture in Baribis Fault possibly related to the 1847 major earthquake event in the Cirebon area. In *IOP Conference Series: Earth and Environmental Science* (Vol. 873, No. 1, p. 012052). IOP Publishing.

[36] Susilo, S., Meilano, I., Wibowo, S. T., Syetiawan, A., Gaol, Y. A. L., Ramdani, D., & Julzarika, A. (2022). Geodetic Strain of the Baribis Fault Zone in West Java, Indonesia. In *IOP Conference Series: Earth and Environmental Science* (Vol. 1109, No. 1, p. 012008). IOP Publishing.

[37] Widiyantoro, S., Supendi, P., Ardianto, A., Baskara, A. W., Bacon, C. A., Damanik, R., ... & Lesmana, A. (2022). Implications for fault locking south of Jakarta from an investigation of seismic activity along the Baribis fault, northwestern Java, Indonesia. *Scientific reports,* 12(1), 10143.

[38] Ming, Y., Niu, X., Xie, X., Han, Z., Li, Q., & Sun, S. (2021, February). Application of gravity exploration in urban active fault detection. In *IOP Conference Series: Earth and Environmental Science* (Vol. 660, No. 1, p. 012057). IOP Publishing.